Dielectric Relaxation and Far-Infrared Spectroscopic Study of Cation-Site Interactions in Oxide Glasses

ARTICLE *in* THE JOURNAL OF PHYSICAL CHEMISTRY B · MAY 2001

Impact Factor: 3.3 · DOI: 10.1021/jp004438x

6 AUTHORS, INCLUDING:

Christos Varsamis
Technological Educational Institute of Piraeus
69 PUBLICATIONS **812** CITATIONS
SEE PROFILE

Efstratios I. Kamitsos
National Hellenic Research Foundation
195 PUBLICATIONS **3,978** CITATIONS
SEE PROFILE

Jean-Charles Giuntini
Université de Montpellier
125 PUBLICATIONS **1,216** CITATIONS
SEE PROFILE

Dielectric Relaxation and Far-Infrared Spectroscopic Study of Cation-Site Interactions in Oxide Glasses

S. Devautour,*,† C. P. E. Varsamis,‡ F. Henn,† E. I. Kamitsos,‡ J. C. Giuntini,† and J. Vanderschueren§,||

Laboratoire de Physico-Chimie de la Matière Condensée, UMR CNRS 5617, Université de Montpellier II, Place Eugène Bataillon, F-34095 Montpellier Cedex 5, France, Theoretical and Physical Chemistry Institute, National Hellenic Research Foundation, 48 Vass. Constantinou avenue, G-11635 Athens, Greece, and Laboratoire de Chimie Macromoléculaire et de Chimie Physique, Research Associate of the National Fund for Scientific Research Université de Liège, Institut de Chimie au Sart Tilman, B-4000 Liège, Belgium

Received: December 7, 2000; In Final Form: March 21, 2001

Alkali triborate glasses $M_2O{\cdot}3B_2O_3$, with M = Li, Na, K, Rb, and Cs, have been investigated by dielectric relaxation spectroscopy employing two different experimental techniques, i.e., complex impedance spectroscopy (CIS) and the thermally stimulated current (TSC) technique. The results of these two dielectric spectroscopies can be fruitfully analyzed in terms of distribution functions of relaxation times and favorably compared. The dielectric results are discussed by analyzing the far-infrared absorption profiles due to the localized metal cation site vibrations. Both dielectric and far-infrared spectroscopies show that metal cations are embedded in at least two or three types of network sites. The activation energies for cation detrapping and for ionic mobility were also evaluated.

1. Introduction

The structure of ionic oxide glasses (e.g., alkali silicates and borates) has been the subject of numerous investigations using a range of experimental and theoretical techniques including vibrational spectroscopy,[1−4] NMR,[5−9] neutron diffraction,[10,11] X-ray scattering and absorption,[11,12] molecular-dynamics,[9,13,14] and ab initio molecular orbital calculations.[15] In many cases, the nature and population of the local structural polyhedra which constitute the glass network can be revealed.[1−12] However, a detailed description of network sites hosting the metal cations in glass is still a subject with many open questions. Infrared spectroscopy provides the means to investigate cation sites in ionic glasses, because localized metal-cation-site vibrational modes are active in the far-infrared spectral range.[1−4,15,16] In most ionic oxide glasses, the analysis of the asymmetric far-infrared profiles strongly supports the existence of at least two distinct distributions of sites hosting metal cations.[2,4,16] This "two-site" model was interpreted on the basis of the chemical versatility of glassy networks to provide sites for metal ions with variable coordination number and anionic charge density.[16] In a different approach, the entire cation-site vibrational activity in the far-infrared was attributed to a single type of sodium ion sites in borate glasses.[15] Besides infrared spectroscopy, a novel solid-state 2d heteronuclear correlation NMR experiment provided evidence for the existence of multiple sodium sites in mixed Li/Na phosphate glasses.[8] Recently, combined ^{23}Na multiple-quantum magic-angle spinning NMR experiments with molecular dynamics studies showed the existence of several types of sodium sites in binary and ternary sodium silicate glasses.[9]

It is recognized that a deeper knowledge of the cation-site interactions is required to understand many macroscopic properties of glasses including ionic transport, basicity and operation of color centers. For example, a close relation between cation-site vibration frequency and optical basicity has been established for alkali- and alkaline earth-borate glasses.[17,18] Also, theoretical models for ion transport in glasses involving preferred pathways,[19] site memory effects,[20] or cation microsegregation[21] are based on the existence of distinct cation sites. Along these lines, it was proposed by Ingram[22] that a "two-site" model is a consequence of a conductivity mechanism which focuses attention on the dynamics of the site relaxation process. Moreover, a close correlation was found between the frequency of the localized cation-site vibration and the activation energy for ionic transport in rubidium germanate glasses.[23]

The aim of this paper is to demonstrate that an alternative efficient tool to investigate cation sites and to determine the cation-network interaction energy in glasses is the combination of dielectric relaxation and far-infrared spectroscopies. In fact, previous works showed that dielectric spectroscopy, with suitable experimental setup[24] and procedures,[25] can be applied to obtain a proper dipolar response of the material in the experimental dielectric signal. This response can be regarded as originating from a dipolar reorientation involving an ionic hopping mechanism within short distances. Consequently, one can yield useful information on both the distribution of cation sites and the cation-network interaction energy. This dielectric approach has been applied to crystalline aluminosilicate materials, like zeolites and clay minerals, and the results were found to compare successfully with those obtained from the analysis of X-ray diffraction data. In particular, the dielectric study of mordenite type zeolites gave quantitative data in close agreement

* To whom correspondence should be addressed. E-mail: devaut@lpmc.univ-montp2.fr. Fax: 33 4 67 14 42 90.
† Laboratoire de Physico-Chimie de la Matière Condensée.
‡ Theoretical and Physical Chemistry Institute.
§ Laboratoire de Chimie Macromoléculaire et de Chimie Physique
|| Deceased. This paper is dedicated to his memory.

10.1021/jp004438x CCC: $20.00
Published on Web 05/30/2001

with the crystallographic ones, such as (i) the number and type of sites occupied by the charge compensating metal cations, (ii) the degree of occupancy of each site, and (iii) the interaction energy between charge carriers and the zeolitic network.[26,27]

The lack of long range order in glasses restricts the effectiveness of X-ray techniques for local structural evaluation. Therefore, dielectric relaxation spectroscopy appears as a promising method to probe and evaluate the local environments of metal cations in glass. In this work we show for the first time that properly collected and analyzed dielectric relaxation data can be compared favorably with results of far-infrared spectroscopy. This combined approach of dielectric and infrared spectroscopy is applied here to alkali triborate glasses, $M_2O\cdot 3B_2O_3$ (M = alkali metal). The choice of this system was motivated by the fact that stable glass samples can be prepared in forms suitable for dielectric and infrared spectroscopic measurements.

2. Dielectric Relaxation

As mentioned above, dielectric relaxation in ionic conducting solids can be regarded as a dipolar reorientation phenomenon. This reorientation process is usually associated with an ionic hopping mechanism operating within short distances, and characterized by a relaxation time τ. This hopping mechanism is thermally activated such as the relaxation time τ is associated with an energy barrier ΔE

$$\tau = \tau_0 \exp\left(\frac{\Delta E}{kT}\right) \qquad \text{with} \qquad \tau_0 = \tau^*_0 \exp\left(\frac{\Delta S}{k}\right) \quad (1)$$

where k is the Boltzmann constant, T is the temperature, τ^*_0 is the inverse of the characteristic vibration frequency of the charge carrier trapped in its site, and ΔS is the entropy variation associated with the reorientation mechanism. Basically, in the experimentally explored temperature domains the variations of the entropy are assumed to be negligible, when the dielectric response of cations in similar environments are compared. Consequently, τ_0 can be associated, to a first approximation, with the cation-site vibration frequency evaluated from far-infrared spectra.

To measure the proper dielectric response of an ionic conductor, it is necessary to compare results obtained from at least two different techniques. This is because the application of an electrical field to an ionic conductor creates nondipolar phenomena (i.e., dc conductivity, electrode polarization, and interfacial effects), and these phenomena partially overlap and screen the pure dielectric response of the material. To the best of our knowledge, such comparisons between different dielectric results are not often made in ionic solids, and this complicates both data analysis and interpretation of results. In this work, we combine complex impedance spectroscopy (CIS) and thermally stimulated current measurements (TSC) to evaluate the dielectric response in typical ionic oxide glasses.

Assuming the occurrence of a distribution of relaxation times, we can analyze the dielectric relaxation results in terms of the dielectric relaxation loss spectrum $\epsilon''(\omega,T)$, measured by CIS as a function of frequency and temperature, and the thermally stimulated depolarization current $I(T)$, collected in TSC by applying a linear heating ramp, i.e., $T = T_0 + qt$. Provided that the pure dielectric response can be extracted from the experimental signals, the quantities $\epsilon''(\omega,T)$ and $I(T)$ are given by the following equations:

$$\epsilon''(\omega,T) = [\epsilon_s(T) - \epsilon_\infty(T)] \int_{\ln(\tau_0)}^{\ln(\tau_\infty)} G_{CIS}(\tau) \frac{\omega\tau}{1+\omega^2\tau^2} d(\ln \tau) \quad (2)$$

$$I(T) = P_0 \sum^{i} \frac{G_{TSC}(\tau_i)}{\tau_i} \exp\left[-{}^1\!/_q \int_{T_0}^{T} \frac{1}{\tau_i} dT\right] \quad (3)$$

where ϵ_s and ϵ_∞ are the permittivities measured at $\omega\tau \ll 1$ and $\omega\tau \gg 1$, respectively. By normalizing the distribution functions of relaxation time, such as

$$\int_{\ln(\tau_0)}^{\ln(\tau_\infty)} G_{CIS}(\tau)\, d(\ln \tau) = \int_{\ln(\tau_0)}^{\ln(\tau_\infty)} G_{TSC}(\tau)\, d(\ln \tau) \quad (4)$$

$G_{CIS}(\tau)$ and $G_{TSC}(\tau)$ should be comparable and therefore considered as intrinsic features of the material. Basically, $G_{CIS}(\tau)$ and $G_{TSC}(\tau)$ can be obtained by using "inverse method" or by applying a fitting procedure described elsewhere.[28] The inversion of eqs 2 and 3 is by definition a so-called "ill posed problem".[29,30] It means that there is no unique solution. Therefore, one limits the error on the determination of $G(\tau)$ by making a strict comparison between $G(\tau)_{TSC}$ and $G(\tau)_{CIS}$, which must have the similar shape.

3. Experimental Section

Stoichiometric amounts of metal carbonates, M_2CO_3 (M = alkali), and B_2O_3 powders were mixed well and melted in Pt crucibles for 30 min at ca. 1000 °C. Glasses were obtained in cylindrical forms by casting the bubble-free melt in a stainless steel mold, and subsequent annealing at ca. 10 °C below the glass transition temperature. Specimens for infrared and dielectric measurements were prepared by cutting and polishing the glass samples to obtain disks of 10 mm in diameter and 1 mm in thickness (with an accuracy of ± 10 μm).

Infrared specular reflectance spectra were recorded at room temperature in a quasi normal incidence mode (11°), on a Fourier transform vacuum spectrometer (Bruker IFS 133v) covering the range 25−4000 cm^{-1}. The reflectance data were analyzed by the usual Kramers−Kronig transformation to yield the absorption coefficient spectra presented in this work.

Prior to the CIS and TSC measurements, the samples were kept under a dry nitrogen atmosphere at 200 °C for 2 h to remove any residual humidity. CIS polarization conductivity measurements were made between 10^{-1} and 10^6 Hz, in the temperature range 220−240 °C, using a Novocontrol alpha analyzer impedance meter. TSC experiments were performed under helium in a Solomat TSC/RMA spectrometer (model 91000+). The samples were first polarized at 100 °C under the application of a 300 V cm^{-1} dc field and were subsequently cooled to −160 °C. At this temperature the dc electrical field was switched off, and the depolarization current was then recorded by heating the system with a 7 °C/min linear rate. For both CIS and TSC measurements, the glass samples were inserted between two PTFE films, of 10 μm of thickness, to avoid direct charge injection, electrode polarization and diffusion effects.

4. Results and Discussion

4.1. Dielectric Relaxation Results. The measured dielectric spectra of $M_2O\cdot 3B_2O_3$ glasses are presented in terms of the imaginary part of the permittivity losses $\epsilon''(\omega,T)$ and the depolarization current $I(T)$. For such systems, the dielectric response is ascribed to the reorientation motion of dipoles

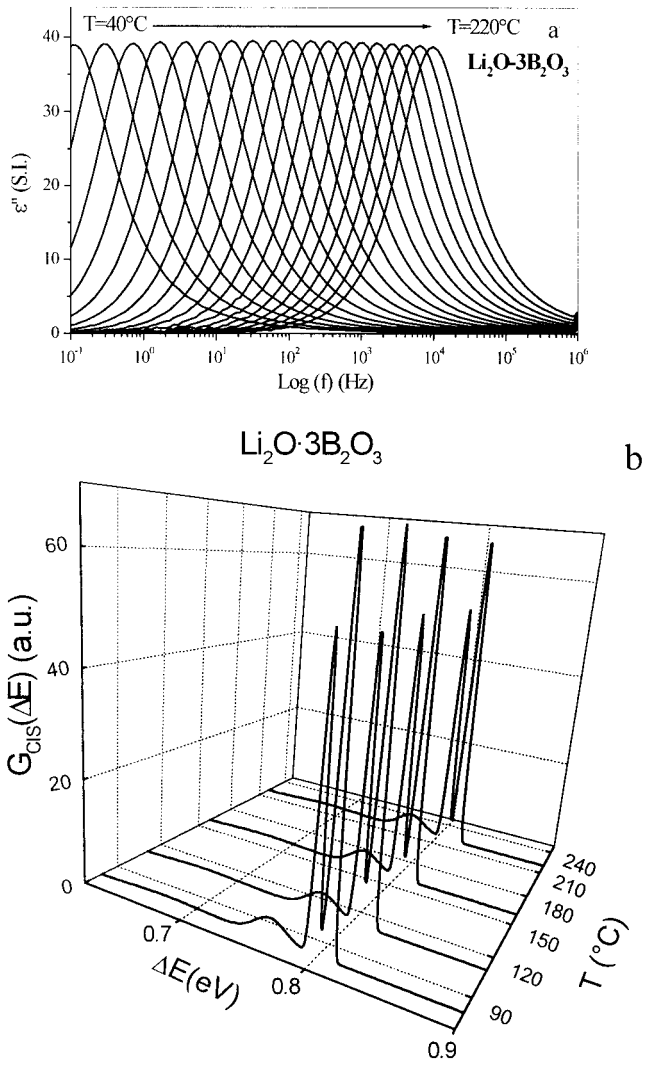

Figure 1. (a) Temperature dependence of the imaginary part of the permittivity loss spectrum $\epsilon''(\omega)$ (b) and of the corresponding distribution function in energy $G_{CIS}(\Delta E)$ for the $Li_2O{\cdot}3B_2O_3$ glass.

constituted by the alkali metal ion and its negatively charged site, which is formed by oxygen atoms of the borate network.

Figure 1a presents typical $\epsilon''(\omega,T)$ spectra for the lithium triborate glass, and shows that the experimental peak shifts toward higher frequencies upon increasing temperature. The same trend was observed for all glass compositions investigated in this work. The corresponding distribution functions in energy $G_{CIS}(\Delta E)$ were obtained by fitting the experimental data with eq 2, and are plotted for different temperatures in Figure 1b. It is evident that, within the errors introduced by experimental and data analysis procedures (estimated at around ±1%), the shape and the position in energy of the distribution functions are almost temperature independent. On these grounds, we can make comparisons of $G_{CIS}(\Delta E)$ for different glasses even at different temperatures. Figure 2 compiles $G_{CIS}(\Delta E)$ curves obtained for all alkali triborate glasses. It is clear that the shape and the position in energy of such curves depend strongly on cation nature in a rather systematic way, and in particular the following sequence holds: $\Delta E_{Li^+} < \Delta E_{Cs^+} < \Delta E_{Rb^+} < \Delta E_{K^+} < \Delta E_{Na^+}$, where ΔE_{i+} refers to the center of gravity of the $G_{CIS}(\Delta E)$ curve.

The evolution with temperature of the depolarization current $I(T)$ and the corresponding distribution function $G_{TSC}(\Delta E)$ for the $K_2O{\cdot}3B_2O_3$ glass are depicted in Figure 3a,b, respectively, and demonstrate the typical behavior of alkali triborate glasses.

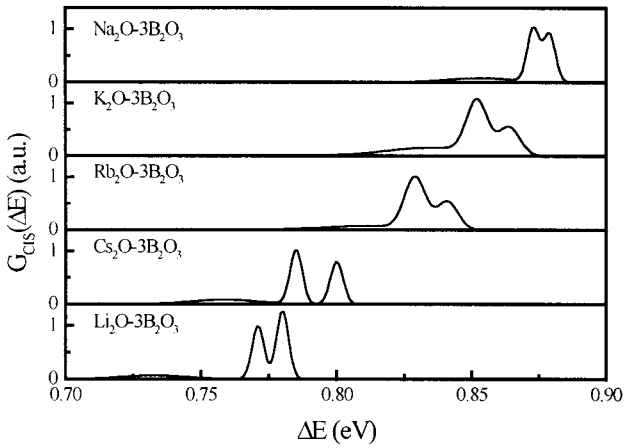

Figure 2. Cation dependence of the distribution in energy $G_{CIS}(\Delta E)$ at $T = 200$ °C for triborate glasses $M_2O{\cdot}3B_2O_3$, where M is alkali metal.

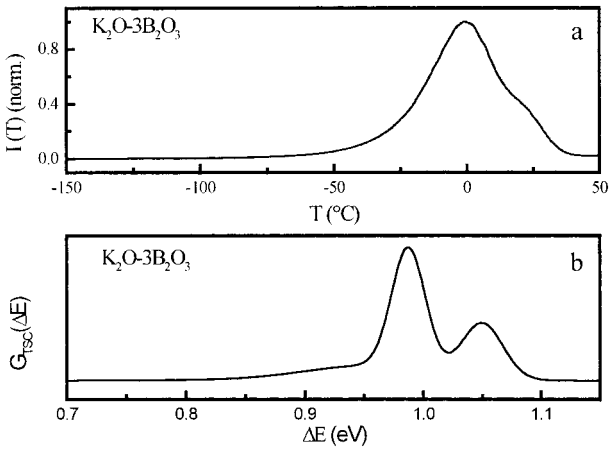

Figure 3. (a) Evolution with temperature of the depolarization current I(T) and (b) the corresponding distribution in energy $G_{TSC}(\Delta E)$ for $K_2O{\cdot}3B_2O_3$ glasses.

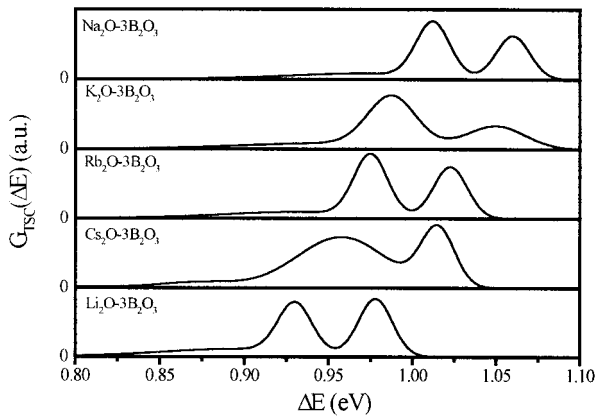

Figure 4. Cation dependence of the $G_{TSC}(\Delta E)$ distribution in $M_2O{\cdot}3B_2O_3$ glasses, where M is alkali metal.

It is noted that the analysis of the depolarization current has been made after removing space charge effects as described elsewhere.[25] The distribution functions obtained by TSC for the alkali triborate glasses are compared in Figure 4 and show the trend $\Delta E_{Li^+} < \Delta E_{Cs^+} < \Delta E_{Rb^+} < \Delta E_{K^+} < \Delta E_{Na^+}$, in full agreement with the CIS results. Thus, both CIS and TSC techniques yield consistent results at least as far as the dependence of the position of the distribution function on the alkali ion is concerned.

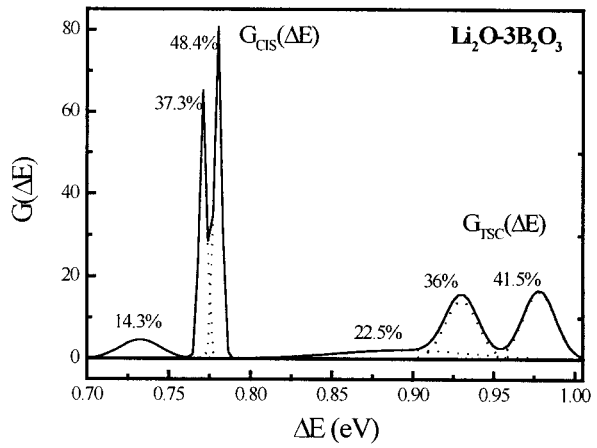

Figure 5. Comparison of normalized $G_{CIS}(\Delta E)$ with $G_{TSC}(\Delta E)$ distribution functions for the $Li_2O{\cdot}3B_2O_3$ glass.

It is now interesting to compare further the results of the two dielectric techniques and obtain additional information on the factors affecting the energy distribution functions. The consideration of both techniques is essential because problems faced with one method can be handled by using the other. In particular, we have already shown that TSC is well adapted for eliminating nondipolar effects in the experimental signal, whereas this is not the case for the CIS technique.[25] However, because of the nonisothermal conditions inherent to the TSC technique, a shift toward higher energy values and a peak broadening of $G_{TSC}(\Delta E)$ is observed with respect to the corresponding $G_{CIS}(\Delta E)$ function of the same material. This is evident in Figure 5 for the $Li_2O{\cdot}3B_2O_3$ glass, and similar effects were also observed for the other glass compositions. On the other hand, TSC appears to be more sensitive in the energy separation of the different contributions resulting from the distribution of cationic sites, but the corresponding energy values are less accurate compared to those of the CIS technique. The latter method exhibits a rather poor energy separation of the different contributions, but enables the determination of the true energy values. Nevertheless, and despite the fact that it is not possible to compare strictly the $G_{CIS}(\Delta E)$ and $G_{TSC}(\Delta E)$ energy distribution curves, they exhibit similar shapes and the same dependence of activation energy on alkali cation. These findings suggest strongly that the same phenomena are involved in both techniques.

It was found that for all triborate glasses the $G_{CIS}(\Delta E)$ and $G_{TSC}(\Delta E)$ curves are deconvoluted into at least three Gaussian components,[31] indicating the existence of three different distributions of cation hosting sites. As shown in Figure 5 for the $Li_2O{\cdot}3B_2O_3$ glass, the contribution of corresponding components of the CIS and TSC distribution functions are quite similar. This result provides additional support to the idea that both techniques probe the same dielectric response mechanisms.[24]

4.2. Far-Infrared Spectroscopic Results. The far-infrared absorption spectra of alkali triborate glasses are shown in Figures 6 and 7. All spectra are found to exhibit characteristic asymmetric profiles, indicating a distribution of cation hosting sites.[16,32] Spectral deconvolution in terms of a distribution function of vibration energies requires at least two Gaussian components when M = K, Rb, or Cs, and these are denoted by H and L for the high and low frequency component, respectively (Figure 6). In the case of Li- and Na-triborate glasses an additional weak component at very low frequency, denoted by VL, was required to improve the agreement between simulated and experimental far-infrared profiles (Figure 7). This VL component could not be unambiguously resolved in the case of K-, Rb-, and Cs-triborate glasses, and this could be due to the

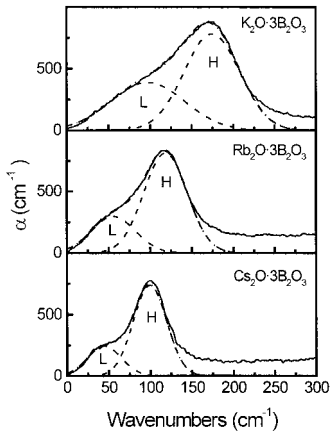

Figure 6. Far-infrared absorption coefficient spectra of $M_2O{\cdot}3B_2O_3$ glasses (M = K, Rb, or Cs). The deconvolution into Gaussian component bands is also shown.

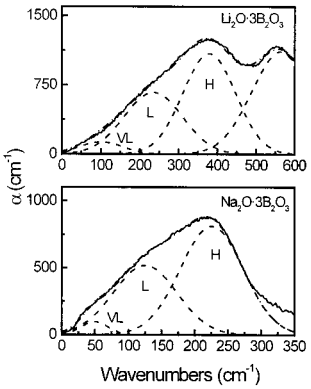

Figure 7. Far-infrared absorption coefficient spectra of $M_2O{\cdot}3B_2O_3$ glasses (M = Li or Na). The deconvolution into Gaussian component bands is also shown.

shift of the corresponding L and H bands toward lower frequencies with increasing cation mass, resulting in strong overlapping with any additional weak component.

In Figure 8a are plotted the frequencies ν_H, ν_L vs the inverse square root of alkali cation mass, $M_C^{-1/2}$. The observed linear correlation suggests that both H and L bands should originate from vibrational modes involving motion of metal cations against their network sites. In the same figure are included the ν_{VL} frequencies obtained for the Li- and Na-triborate glasses. Despite the limited number of these data, the fact that their line tends to zero when the cation mass tends to infinity suggests that the VL component could also originate from cation-site vibrations. Thus, the analysis of far-infrared profiles indicates that Li and Na cations may be embedded into three different distributions of sites, whereas for K, Rb, and Cs ions at least two different environments exist, without excluding the presence of a third type of site.

Recently, the molecular dynamics technique was applied to investigate the nature of the local coordination environments of Li ions in Li-borate glasses, and the results regarding the Li-site energetics were compared with those of far-infrared spectroscopy.[33] It was shown that at least two distinct types of Li sites could be distinguished; with one type of site being formed primarily by nonbridging oxygen atoms in charged borate triangles, e.g., $B\varnothing_2O^-$ (where $\varnothing$ indicates a bridging oxygen atom), but involving also bridging oxygen atoms in neutral borate units, $B\varnothing_3$. Such sites are designated as nonbridging type sites, with their lithium ions denoted by Li^{nb}. In the second type of sites Li ions are coordinated mainly by

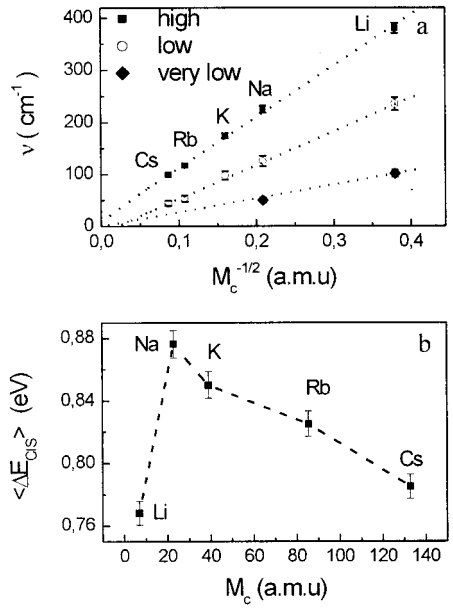

Figure 8. a: Metal-ion-site vibration frequencies vs the inverse square root of cation mass, $M_c^{-1/2}$. By ν_L, ν_H, and ν_{VL} are denoted center frequency values for the deconvoluted far-infrared component bands (see Figures 6 and 7). Lines are least-squares fitting. (b) Evolution of the mean value of CIS cation energy vs alkali cation mass M_c.

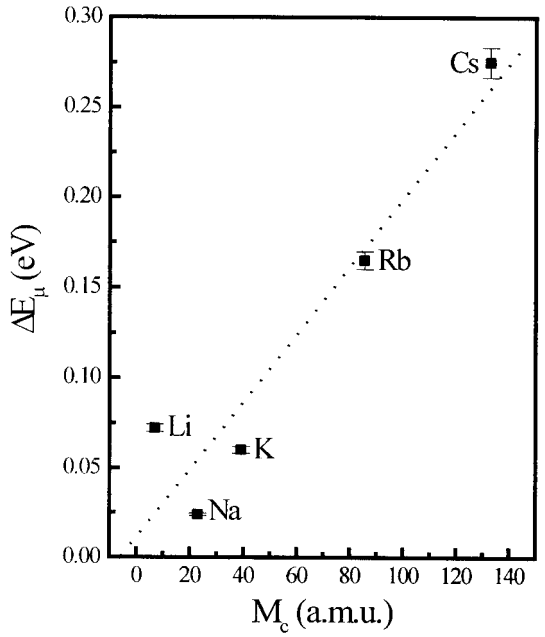

Figure 9. Mean value of the activation energy for cation mobility ΔE_μ as a function of cation mass M_c. Line is least-squares fitting.

bridging-oxygen atoms in charged borate tetrahedra, $B\varnothing_4^-$, and oxygen atoms in $B\varnothing_3$ units. These sites were called bridging-type sites and their lithium ion occupants were denoted by Li^b. It was also shown that the calculated power spectra of Li^{nb} cations are closely associated with the H component in the far-infrared, while the L spectral component can be attributed to vibrations of Li^b cations in their sites.[33] However, the molecular dynamics results do not allow at present a clear assessment of the origin of the weak VL component band. A tentative attribution of the VL band to Li ions in sites of low charge density may not be unrealistic. Regarding this point we note that even for binary silicate glasses (e.g., $Na_2O{\cdot}5SiO_2$), where the formal negative charge is located only on nonbridging oxygens, two types of Na ions were identified. Sodium ions associated mainly with sites of nonbridging oxygens were considered as modifier ions, and were found to account for ca. 73% of the total Na-ion population.[9]

4.3. Comparison of Dielectric Relaxation with Far-Infrared Results. Although the dielectric relaxation and far-infrared experimental approaches are different, it is possible to treat the experimental data obtained in both cases in terms of distribution functions characterizing the interaction energy between the alkali cation and its hosting site. Therefore, both techniques can probe the local environments of alkali ions in the glassy network.

The present results lead to the conclusion that the deconvolution procedures applied to analyze the data of each technique converge to the existence of at least two different distributions of cation sites in alkali triborate glasses. In addition to that, attention should be paid to the value of the interaction energy as a function of metal cation. In the far-infrared analysis, the increasing linear dependence of both ν_L and ν_H on the inverse square root of cation mass $M_C^{-1/2}$ (see Figure 8a) suggests that the corresponding vibration energy decreases continuously upon increasing the cation mass. The same trend is found in the dielectric relaxation data for all alkali triborate glasses except for Li-triborate. This is shown in Figure 8b where the interaction energy ΔE_{CIS} (considered as a mean energy value of the global distribution function $G_{CIS}(\Delta E)$) is plotted as a function of the alkali mass. The peculiar behavior of the Li^+ cation is clearly observed in this case. A similar behavior was found in faujasite zeolite type systems,[34,35] and was attributed to the exceptional hardness of the Li^+ cation.[36]

4.4. Comparison of Dielectric Relaxation with Conductivity Results. It was shown previously[32] that the activation energy for σ_{dc} shows a regular cation dependence in alkali triborate glasses, with no sign for a peculiar behavior of Li^+ cation. Following the well-known relation $\sigma = n\mu e$, where n is the number of the charge carrier, μ is its mobility, and e is the charge, the activation energy $\Delta E(\sigma_{dc})$ can be decomposed into two terms; one related to the activation energy required for detrapping the cation from its hosting site ΔE_c, and the other characterizing the cation mobility ΔE_μ, such as

$$\Delta E(\sigma_{dc}) = \Delta E_c + \Delta E_\mu \quad (5)$$

Since ΔE_c represents the detrapping energy involved in the local reorientation process, it must be closely related to the dielectric relaxation mean energy value obtained by CIS, $\langle \Delta E_{CIS} \rangle$. Therefore, from the known $\Delta E(\sigma_{dc})$ and ΔE_c values it is possible to estimate also the mobility contribution term ΔE_μ.

The evolution of ΔE_μ with cation mass M_C, is illustrated in Figure 9. Contrary to the trend of $\langle \Delta E_{CIS} \rangle$, it is found that ΔE_μ depends almost linearly on cation mass and tends to zero when M_C tends also to zero. This finding suggests that the activation energy required for ionic conductivity in glass is not due only to the creation of free cations, as suggested by the weak electrolyte model, nor to ion mobility alone as predicted by the strong electrolyte theory. Our results show that both detrapping and mobility phenomena participate in the ion conduction process, with their individual contributions showing strong cation dependence. Moreover, it is interesting to note that the ΔE_μ values are of the same order of magnitude as found for Na^+ in quartz.[37]

5. Conclusions

We have demonstrated that a proper determination of the true dielectric relaxation properties in an ionic solid requires the

comparison of the results obtained through two different dielectric techniques. In the present study, complex impedance spectroscopy (CIS) and thermally stimulated current (TSC) experimental techniques have been employed.

It was further shown that the use of a distribution function of energies in analyzing dielectric relaxation data leads to valuable information concerning the number of different distributions of sites hosting the ionic charge carriers. A similar approach of distribution functions is adopted in analyzing the data of far-infrared spectroscopy. Thus, a direct comparison can be made between the results obtained through dielectric relaxation and far-infrared spectroscopy, although different ionic motions and related energies are probed by these techniques.

The comparative study of $M_2O{\cdot}3B_2O_3$ glasses points toward similar conclusions concerning the distributions of local sites hosting the alkali metal ions in these glasses. In particular, it was found that alkali ions are embedded into at least two different types of sites formed by the borate network.

Finally, by comparing activation energies obtained from CIS and dc conductivity data, it was possible to access the mobility term ΔE_μ involved in the total activation energy $\Delta E(\sigma_{dc})$ required for ionic conduction in glasses. For the alkali triborate family, the ΔE_μ energy term was found to depend linearly on alkali cation mass.

Acknowledgment. Partial support of this work by the Greek−French bilateral R&D program (PLATON project) is gratefully acknowledged.

References and Notes

(1) Merzbacher, C. I.; White, W. B. *J. Non-Cryst. Solids* **1991**, *130*, 18.
(2) Kamitsos, E. I.; Patsis, A. P.; Chryssikos, G. D. *J. Non-Cryst. Solids* **1993**, *152*, 246.
(3) Parot-Rajaona, T.; Cote, B.; Bessada, C.; Massiot, D.; Gervais, F. *J. Non-Cryst. Solids* **1994**, *169*, 1.
(4) Varsamis, C. P.; Kamitsos, E. I.; Chryssikos, G. D. *Phys. Rev. B* **1999**, *60*, 3885.
(5) Zhong, J.; Bray, P. J. *J. Non-Cryst. Solids* **1989**, *111*, 67.
(6) Maekawa, H.; Maekawa, T.; Kawamura, K.; Yokokawa, T. *J. Non-Cryst. Solids* **1991**, 127, 53.
(7) Ratai, E.; Janssen, M.; Eckert, H. *Solid State Ionics* **1998**, *105*, 25.
(8) Wenslow, R. M.; Mueller, K. T. *J. Non-Cryst. Solids* **1998**, *231*, 78.
(9) Angeli, F.; Delaye, J.-M.; Charpentier, T.; Petit, J.-C.; Ghaleb, D.; Faucon, P. *J. Non-Cryst. Solids* **2000**, *276*, 132.
(10) Rocca, F.; Dalba, G.; Fornasini, P.; Tomasi, A. *Solid State Ionics* **1992**, *53*−*56*, 1253.
(11) Swenson, J.; Borjesson, L.; Howells, W. S. *Phys. Rev. B* **1995**, *52*, 9310.
(12) Swenson, J.; Borjesson, L.; McGreevy, R. L.; Howells, W. S. *Phys. Rev. B* **1997**, 55, 11236.
(13) Anderson, D. C.; Kieffer, J.; Klarsfeld, S. *J. Chem. Phys* **1993**, *98*, 8978.
(14) Park, B.; Cormack, A. N. *J. Non-Cryst. Solids* **1999**, *255*, 112.
(15) Uchino, T.; Yoko, T. In *Borate Glasses, Crystals and Melts*; Wright, A. C., Feller, S. A., Hannon, A. C., Eds.; Alden Press: Oxford, UK 1997; pp 417−424.
(16) Kamitsos, E. I.; Chryssikos, G. D. *Solid State Ionics* **1998**, *105*, 75.
(17) Kamitsos, E. I.; Chryssikos, G. D.; Patsis, A. P.; Duffy, J. A. *J. Non-Cryst. Solids* **1996**, *196*, 249.
(18) Duffy, J. A.; Harris, B.; Kamitsos, E. I.; Chryssikos, G. D.; Yiannopoulos, Y. D. *J. Phys. Chem. B* **1997**, *101*, 4188.
(19) Ingram, M. D.; Mackenzie, M. A.; Muller, W.; Torge, M. *Solid State Ionics* **1988**, *28*−*30*, 677.
(20) Maas, P.; Bunde, A.; Ingram, M. D. *Phys. Rev. Lett.* **1992**, *68*, 3064.
(21) Greaves, G. N.; Ngai, K. L. *Phys. Rev. B* **1995**, *52*, 6358.
(22) Ingram, M. D. *J. Non-Cryst. Solids* **1997**, *222*, 42.
(23) Kamitsos, E. I.; Yiannopoulos, Y. D.; Jain, H.; Huang, W. C. *J. Non-Cryst. Solids* **1996**, *203*, 312.
(24) Henn, F.; Devautour, S.; Maati, L.; Giuntini, J. C.; Schaefer, H.; Zanchetta, J. V.; Vanderschueren, J. *Solid States Ionics* **2000**, 136−137, 1335.
(25) Devautour, S.; Henn, F.; Giuntini, J. C.; Zanchetta, J. V.; Vanderschueren, J. *J. Phys. D: Appl. Phys*. **1999**, *32*, 147.
(26) Devautour, S.; Vanderschueren, J.; Giuntini, J. C.; Henn, F.; Zanchetta, J. V.; Ginoux, J. L. *J. Phys. Chem. B* **1998**, *102*, 3749.
(27) Devautour, S.; Giuntini, J. C.; Henn, F.; Douillard, J. M.; Zanchetta, J. V.; Vanderschueren, J. *J. Phys. Chem. B* **1999**, *103*, 3275.
(28) Devautour, S.; Vanderschueren, J.; Giuntini, J. C.; Henn, F.; Zanchetta, J. V *J. Appl. Phys.* **1997**, *82*, 5057.
(29) Schäfer, H.; Sternin, E. *La Physique au Canada* **1997**, March-April, 77.
(30) Devautour, S.; Schäfer, H.; Giuntini, J. C.; Henn, F.; Zanchetta, J. V. *Ionics* **1997**, 3 373.
(31) Landau, L.; Lifchitz, E. *Physique statistique*; MIR Ed.; Moscow, 1967.
(32) Chryssikos, G. D.; Liu, L.; Varsamis, C. P.; Kamitsos, E. I. *J. Non-Cryst. Sol.* **1998**, 235−237, 761.
(33) Varsamis, C. P. E.; Vegiri, A.; Kamitsos, E. I. *Condensed Matter Phys.* **2001**, *4*, 1.
(34) Kalogeras, J. M.; Vassilikou-Dova, A. *Cryst. Res. Technol*. **1996**, *31*−*36*, 693.
(35) Kalogeras, J. M.; Vassilikou-Dova, A. *Electrical Properties of Zeolitic Catalysts, Defect and Diffusion Forum*; Fisher, D. J., Ed.; Scitec Publications Ltd: Switzerland, 1998; Vol.164.
(36) Xu, S.; Harsh, J. B. *Soil Sci. Soc. Am.* **1990**, *54*, 357.
(37) Jain, H.; Nowick, A. S. *J. Appl. Phys.* **1982**, *53*, 485.